

**Experimental characterization of quantum polarization of three-photon states**Yosep Kim,<sup>1</sup> Gunnar Björk,<sup>2</sup> and Yoon-Ho Kim<sup>1</sup><sup>1</sup>*Department of Physics, Pohang University of Science and Technology (POSTECH), Pohang, 37673, Korea*<sup>2</sup>*Department of Applied Physics, Royal Institute of Technology (KTH), AlbaNova, SE-106 91 Stockholm, Sweden*

(Received 23 June 2017; published 22 September 2017)

We experimentally investigate various quantum polarization features of three-photon quantum states, including product and entangled states with varying purity. The three-photon quantum states are categorized into six classes based on the rotation symmetry of mean, variance, and skewness of the polarization distribution. The representative three-photon quantum states in each category are prepared from double-pair emission from pulsed spontaneous parametric down-conversion and quantum interferometry. We demonstrate that the three-photon quantum states show interesting quantum polarization properties, such as maximum sum-uncertainty and hidden polarizations.

DOI: [10.1103/PhysRevA.96.033840](https://doi.org/10.1103/PhysRevA.96.033840)**I. INTRODUCTION**

The polarization degree of freedom of single photons has been widely used to explore quantum phenomena, since polarization-entangled photon pairs can be prepared with high fidelity and the polarization state is easy to manipulate with linear optics. For example, polarization-entangled photons have been utilized for a variety of fundamental tests of quantum physics, including local hidden variables theories [1] and epistemic models of the wave function [2]. In addition, a plethora of quantum information technologies have been experimentally implemented using photon polarization, such as quantum key distribution [3], quantum dense coding [4], quantum teleportation [5], and quantum computing [6].

The polarization state of light is conventionally described through the use of Stokes parameters that can be represented as a polarization direction and a degree of polarization on the Poincaré sphere [7]. Since the Stokes parameters show only the averaged, “classical” features, they are not sufficient to describe the quantum polarization features fully. For instance, there exists “classically” unpolarized light which has nonisotropic second-order polarization, thus making the state polarized [8]. This example highlights the existence of hidden polarization features and the importance of polarization fluctuations. Up to now, various quantum states have been studied, such as squeezed polarization states [9,10] and entangled photon states [11]. In addition, efficient polarization tomography methods have been suggested [12–15].

In this paper, we experimentally investigate various quantum polarization features of three-photon quantum states, including product and entangled states with varying purity. The studied three-photon states are isomorphic to the states of a composite system consisting of three spin-1/2 particles with the bosonic characteristic, that is, the symmetric Hilbert subspace. To fully describe the properties of the states, up to the third-order Stokes parameters are necessary and sufficient, since the fourth- and higher-order polarization moments contain no additional information. Thus, the Stokes parameter characterization is an alternative representation to the usual density matrix representation of any polarization state.

To explain the relation between conventional tomography of multimode states and our method, it is helpful to observe that our method assumes two-mode states where all particles

are measured locally in a single spatial mode. Therefore, our case is different from the case which allows, or even requires, separate measurements of each “particle” or qudit in a multimode state. As an example, take a three-qubit state space spanned by the eight vectors  $|0,0,0\rangle, |0,0,1\rangle, \dots, |1,1,1\rangle$ . This space is mathematically isomorphic to the two-mode, seven-photon polarization state space spanned by the eight vectors  $|0,7\rangle, |1,6\rangle, \dots, |7,0\rangle$ . In principle, any measurement or projection in one space has an equivalent measurement in the other space, but physically such measurements or projections are very different. In the three-qubit space, a natural operation is the measurement of or tracing over one qubit, reducing the space of the remaining two-qubit state to dimension four. This is a very unnatural measurement for a seven-photon polarization state. Likewise, the extreme superposition  $(|0,0,0\rangle + |1,1,1\rangle)/\sqrt{2}$ , that is a GHZ state, has very different properties and applications than the state  $(|7,0\rangle + |0,7\rangle)/\sqrt{2}$ , which is a NOON state [16–18].

A consequence is that tomography through measurement of correlations between local measurements of qubits or qudits has no natural corresponding correlation measurement scheme for polarization states in composite Hilbert space dimensions. In a polarization space of prime dimension, such as a two-mode four-photon state (spanning five dimensions), there is simply no equivalent multimode space since 5 is a prime.

The central moments of the Stokes operator are also useful to describe the polarization distribution on the Poincaré sphere with Gaussian approximation [14]. The mean, variance, and skewness represent the first-, second-, and third-order central moments, respectively. Through their central moments, all three-photon quantum states are categorized into six different classes according to Table I based on their rotation invariance (on the Poincaré sphere) of their the mean, variance, and skewness. In this work, six class-representative three-photon quantum states are experimentally prepared and measured to confirm the predicted polarization properties.

**II. THEORY**

The Stokes parameters consist of the total intensity  $S_0$  and the three elements of Stokes vector  $\vec{S} = (S_1, S_2, S_3)$  which represent complementary polarization directions on

TABLE I. Classification and examples of three-photon quantum polarization based on SU(2) rotation invariance of mean  $\langle \hat{S}_n \rangle$ , variance  $\langle \hat{\Delta}_n^2 \rangle$ , and skewness  $\langle \hat{\Delta}_n^3 \rangle$  [14]. The symbol O indicates rotation invariance of the particular order of quantum polarization.

Rotation invariance <sup>a</sup>			Representative state in each class <sup>b</sup>
$\langle \hat{S}_n \rangle$	$\langle \hat{\Delta}_n^2 \rangle$	$\langle \hat{\Delta}_n^3 \rangle$	
O	O	O	$\hat{1}/4$
O	O	X	$\frac{1}{3} 3,0\rangle\langle 3,0  + \frac{1}{2} 1,2\rangle\langle 1,2  + \frac{1}{6} 0,3\rangle\langle 0,3 $
O	X	O	$\frac{1}{2}( 3,0\rangle\langle 3,0  +  0,3\rangle\langle 0,3 )$
O	X	X	$\frac{1}{\sqrt{2}}( 3,0\rangle - i 0,3\rangle)$
X	O	X	$\frac{19}{36} 3,0\rangle\langle 3,0  + \frac{15}{36} 1,2\rangle\langle 1,2  + \frac{1}{18} 0,3\rangle\langle 0,3 $
X	X	X	$ 3,0\rangle$

<sup>a</sup>For three-photon polarization states, six classes are physically possible among eight possibilities.

<sup>b</sup>Fock states in horizontal and vertical polarization mode.

the Poincaré (or Bloch) sphere. The values of  $(S_1, S_2, S_3)$  are obtained from intensity differences between orthogonal polarizations: diagonal and antidiagonal, right and left circular, and horizontal and vertical polarizations, respectively. By substituting the bosonic number operator for intensity, the Stokes operators can be well defined and they give quantized values of the Stokes parameters. The operators are expressed as [8]

$$\begin{aligned} \hat{S}_0 &= \hat{a}_H^\dagger \hat{a}_H + \hat{a}_V^\dagger \hat{a}_V, & \hat{S}_1 &= \hat{a}_H \hat{a}_V^\dagger + \hat{a}_H^\dagger \hat{a}_V, \\ \hat{S}_2 &= i(\hat{a}_H \hat{a}_V^\dagger - \hat{a}_H^\dagger \hat{a}_V), & \hat{S}_3 &= \hat{a}_H^\dagger \hat{a}_H - \hat{a}_V^\dagger \hat{a}_V, \end{aligned} \quad (1)$$

where  $\hat{a}_H$  ( $\hat{a}_V$ ) is the annihilation operator for the horizontal (vertical) polarization mode. Their commutation relationships can be derived from the bosonic commutation relations between annihilation operators:

$$[\hat{S}_0, \hat{S}_j] = 0, \quad (2a)$$

$$[\hat{S}_j, \hat{S}_k] = i2\epsilon_{jkl}\hat{S}_l, \quad j, k, l \in \{1, 2, 3\}, \quad (2b)$$

where  $\epsilon_{jkl}$  is the Levi-Civita tensor symbol.

The physical properties of the Stokes operators are implied by the commutation relations. As indicated by Eq. (2a), the commutation between the total photon number operator  $\hat{S}_0$  and all other Stokes operators  $\hat{S}_j$  indicates that the Stokes parameters and photon number can be measured independently without mutual disturbance. This allows measurements of the Stokes parameters for specific photon-number states with photon-number resolving detectors. This also implies that any moment of the Stokes operators  $\hat{S}_1$ ,  $\hat{S}_2$ , and  $\hat{S}_3$  can be measured in a similar manner.

Moreover, Eq. (2b) indicates that some Stokes parameters must be uncertain, leading to the following inequalities:

$$\sqrt{\langle \hat{\Delta}_j^2 \rangle} \sqrt{\langle \hat{\Delta}_k^2 \rangle} \geq |\epsilon_{jkl} \langle \hat{S}_l \rangle|, \quad j, k, l \in \{1, 2, 3\}, \quad (3a)$$

$$2\langle \hat{S}_0 \rangle \leq \langle \hat{\Delta}_1^2 \rangle + \langle \hat{\Delta}_2^2 \rangle + \langle \hat{\Delta}_3^2 \rangle \leq \langle \hat{S}_0 \rangle (\langle \hat{S}_0 \rangle + 2), \quad (3b)$$

where  $\Delta_j \equiv \hat{S}_j - \langle \hat{S}_j \rangle$  is the central moment of the Stokes operator  $\hat{S}_j$ . The existence of a photonic quantum state with

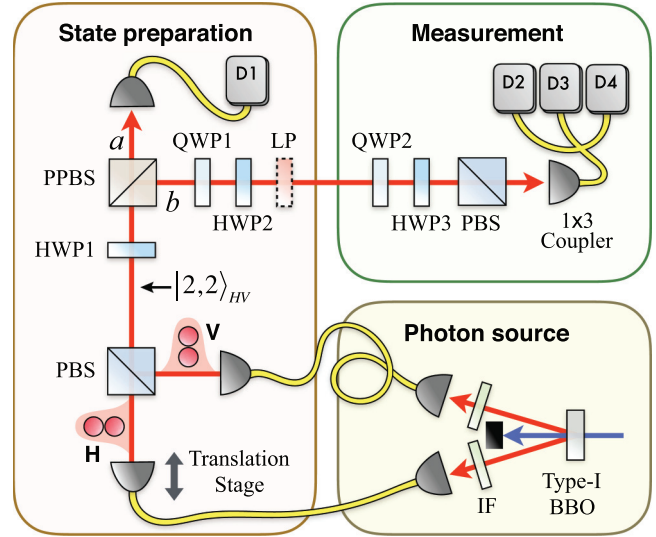


FIG. 1. Experimental scheme for generation and measurement of three-photon states. Two pairs of SPDC photons are sent to an interferometer through single-mode fibers (SMFs) after passing 3-nm bandwidth interference filters (IFs). In the state preparation interferometer, the target states are prepared with a polarizing beam splitter (PBS), a partially polarizing beam splitter (PPBS), half- and quarter-wave plates (HWP, QWP), and a linear polarizer (LP). Conditioned on the detection of a single photon at detector D1, three photons are prepared in mode  $b$  in a particular quantum state set by QWP1, HWP2, and LP. Fourfold coincidence measurements with detectors D1, D2, D3, and D4 for 16 polarization projection measurements allow quantum state tomography for the heralded three-photon states.

hidden polarization, i.e., high-order central moments may have nonzero values even though the state may be first-order unpolarized,  $\langle \hat{S} \rangle = 0$ , is implied in Eq. (3a). Note that Eq. (3b) gives boundaries of the sum of the second-order central moments. For three-photon quantum states, the sum uncertainty is bounded between 6 and 15.

The notion of Stokes operators can be generalized by defining

$$\hat{S}_n = (\hat{S}_1, \hat{S}_2, \hat{S}_3) \cdot \mathbf{n}, \quad (4)$$

where  $\mathbf{n}$  is a unit vector on the Poincaré sphere. The operator  $\hat{S}_n$  assesses the polarization state of the photonic quantum state in the direction  $\mathbf{n}$ . It follows trivially that one can define polarization of order  $m$  in direction  $\mathbf{n}$  as  $\langle \Delta_n^m \rangle$ , where  $\Delta_n \equiv \hat{S}_n - \langle \hat{S}_n \rangle$ .

### III. EXPERIMENT

To confirm the quantum polarization features of three-photon quantum states experimentally, six representative three-photon quantum states are prepared, as shown in Table I. The three-photon states are generated from the double-pair emission of femtosecond-pulse-pumped spontaneous parametric down-conversion (SPDC), see Fig. 1 [17,18]. The pump pulse is derived from a frequency-doubled mode-locked Ti:sapphire laser and has a central wavelength of 390 nm, a pulse duration of 140 fs, and a repetition rate of 80 MHz. The

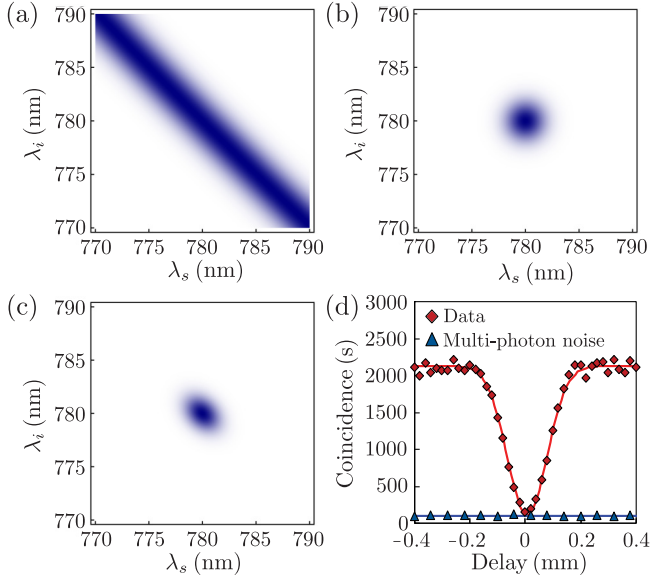


FIG. 2. The simulated joint spectra of (a) SPDC photons, (b) interference filters with 3-nm FWHM bandwidth, and (c) SPDC photons filtered with the interference filters. The simulated joint spectrum in (c) shows that the spectral correlation between the photon pair is well eliminated by the interference filters. (d) The Shih-Alley/Hong-Ou-Mandel interference dip has the visibility of 95.0% (99.6% after multiphoton noise subtraction) at 260-mW pump power, a clear experimental indication that spectral distinguishability between the SPDC photons has been well eliminated by the interference filters. The red solid line is the Gaussian fit to the data. The blue solid line is the linear fit to the calculated multiphoton noise.

SPDC photons, generated from a type-I beta barium borate (BBO) crystal, have a central wavelength of 780 nm and propagate noncollinearly with the pump laser.

To prepare a heralded three-photon quantum state via interference using the scheme in Fig. 1, it is essential that the inherent frequency correlation between the SPDC photon pair be eliminated [19]. In our work, we ensure that this condition is satisfied by using a 0.6-mm-thick type-I BBO crystal, generating broadband SPDC photons, and by filtering the SPDC photons with interference filters (IF) with FWHM of 3 nm. The calculated spectral properties of the unfiltered SPDC photons are shown in Fig. 2(a). It is clear that the SPDC photons from a 0.6-mm-thick type-I BBO crystal have a very broadband emission and show a very strong spectral correlation between the pair. When the SPDC photons are filtered with the 3-nm interference filters [see Fig. 2(b)], the resulting SPDC photons have almost no spectral correlations [see Fig. 2(c)].

The noncollinear, double-pair SPDC photons are combined into a single spatial mode by a polarizing beam splitter (PBS) through single-mode optical fibers for spatial mode cleaning (see Fig. 1). Initially, all four photons are horizontally polarized, but the use of a fiber polarization controller allows us to combine all four photons to a single spatial mode without loss. As all four photons must also be indistinguishable temporally, they all need to arrive at PBS simultaneously. This has been achieved by observing the Shih-Alley/Hong-Ou-Mandel dip between the SPDC photon at the PBS [20,21]. To

observe the two-photon interference dip, the angles of HWP1 and HWP3 are set, respectively, at  $22.5^\circ$  and  $45^\circ$ . All other wave plates, HWP2, QWP1, and QWP2, are set at  $0^\circ$  and LP is removed. The coincidence between detectors D1 and D2 is measured by moving the translation stage on horizontal input mode in Fig. 1. The experimental result shown in Fig. 2(d) exhibits the dip in visibility of 95.0% at 260-mW pump power (99.6% after multiphoton noise subtraction). The translation stage is then set so that the SPDC photons are arriving at the PBS simultaneously. Then, the four-photon quantum state, resulting from the double-pair emission of the SPDC, after the PBS is written as  $|2,2\rangle_{H,V}$ .

We now describe the scheme for heralding a three-photon quantum state in mode  $b$  by detecting a single photon at D1. The initial four-photon state  $|2,2\rangle_{H,V}$  passes through HWP1, and the HWP1 angle ( $0^\circ$  or  $22.5^\circ$ ) is set differently for preparing different three-photon states. Specifically, HWP1 is set at  $0^\circ$  to prepare  $|1,2\rangle$  and  $|2,1\rangle$  and set at  $22.5^\circ$  to prepare  $\frac{1}{\sqrt{2}}(|3,0\rangle - i|0,3\rangle)$ ,  $|3,0\rangle$ , and  $|0,3\rangle$ . After HWP1, the state becomes

$$|HWP1\rangle_{0^\circ} = \frac{1}{2}a_H^\dagger{}^2 a_V^\dagger{}^2 |0\rangle, \quad (5a)$$

$$|HWP1\rangle_{22.5^\circ} = \left( \frac{1}{8}a_H^\dagger{}^4 - \frac{1}{4}a_H^\dagger{}^2 a_V^\dagger{}^2 + \frac{1}{8}a_V^\dagger{}^4 \right) |0\rangle. \quad (5b)$$

The subscripts  $0^\circ$  and  $22.5^\circ$  indicate the angles of HWP1. The photons then impinge on the partially polarizing beam splitter (PPBS) designed for unity reflection for vertical polarization and 1/3 partial reflection for horizontal polarization. Considering the case when one photon is transmitted and found in mode  $a$  and three photons are reflected by the PPBS and found in mode  $b$ , the reflected three-photon state heralded by the presence of a single photon in mode  $a$  is given by

$$|PPBS\rangle_{0^\circ}^b = \frac{1}{\sqrt{2}}a_H^\dagger a_V^\dagger{}^2 |0\rangle, \quad (6a)$$

$$|PPBS\rangle_{22.5^\circ}^b = \left( \frac{1}{9\sqrt{2}}e^{2i\phi}a_H^\dagger{}^3 - \frac{1}{3\sqrt{2}}a_H^\dagger a_V^\dagger{}^2 \right) |0\rangle, \quad (6b)$$

where the phase  $\phi$  comes from the relative phase difference between the two orthogonal polarizations when they are reflected at the PPBS.

The transmitted photon in mode  $a$  is used for heralding of the other three photons by a “click” at detector D1. Then, after the photons pass through QWP1 and HWP2, either both are set at  $0^\circ$  for Eq. (7a) or QWP1 at  $45^\circ$  and HWP2 at  $\phi/4$  for Eq. (7b), the heralded three-photon state becomes

$$|HWP2\rangle_{0^\circ} = \frac{1}{\sqrt{2}}a_H^\dagger a_V^\dagger{}^2 |0\rangle, \quad (7a)$$

$$|HWP2\rangle_{22.5^\circ} = \frac{1}{2\sqrt{3}}(a_H^\dagger{}^3 - i a_V^\dagger{}^3) |0\rangle. \quad (7b)$$

Here, we see that the heralded three-photon states  $|1,2\rangle$  and  $\frac{1}{\sqrt{2}}(|3,0\rangle - i|0,3\rangle)$  have been prepared. The state  $|2,1\rangle$  can be prepared from  $|1,2\rangle$  with the help of HWP2 set at  $45^\circ$ . Also, the states  $|3,0\rangle$  and  $|0,3\rangle$  can be postselected from the entangled state or the NOON state  $\frac{1}{\sqrt{2}}(|3,0\rangle - i|0,3\rangle)$  with a linear polarizer (LP).

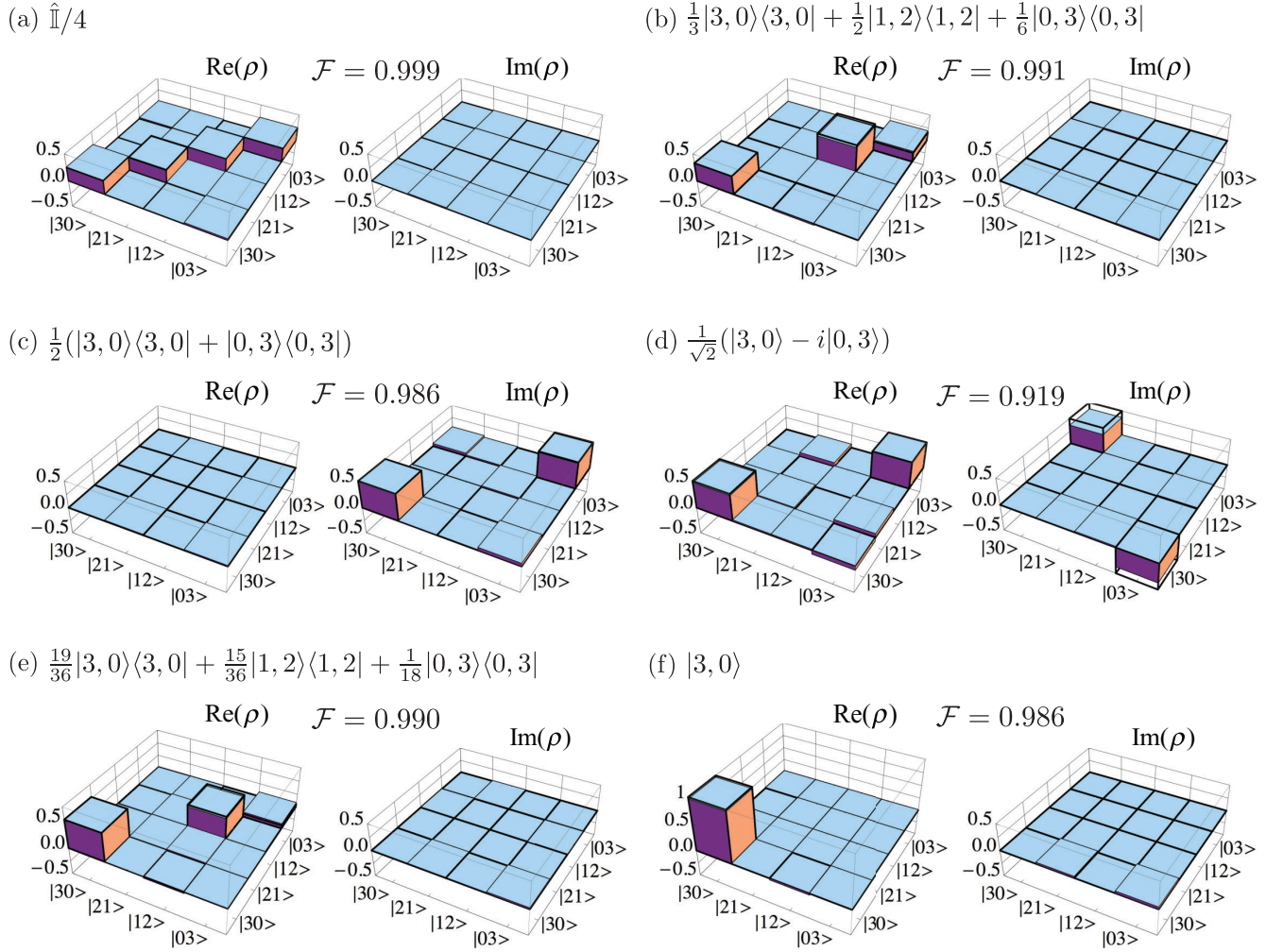


FIG. 3. Density matrices of experimentally prepared heralded three-photon states. Bold lines in the density matrices indicate ideal target density matrices. The fidelity is calculated between the ideal target matrix and the experimentally generated density matrix.

We first measure the value of  $\phi$  experimentally by using the  $|1,1\rangle_{H,V}$  component of the SPDC leading to the coincidence event between detectors D1 and D2. First, HWP1 and QWP1 are set at  $15^\circ$  and  $45^\circ$ , respectively. The photon in mode  $b$  is measured on the projection basis  $\frac{1}{\sqrt{2}}(|H\rangle - |V\rangle)$ . Then, as a function of the HWP2 angle  $\theta$ , the coincidence count between detectors D1 and D2 will be proportional to  $\sin^2\{\frac{1}{2}(\phi - 4\theta)\}$ . Thus, by measuring the angle  $\theta$  at which the coincidence count is minimized, it is possible to determine the phase  $\phi$ . Experimentally, we find that  $\phi = -85.7^\circ$ .

In our scheme, the double-pair event of SPDC contributes to the heralded three-photon state, but triple-pair or higher-order SPDC events lead to multiphoton noise, as they can also trigger the four-photon coincidence circuit. As  $N$ -pair events of SPDC with  $N \geq 3$  increase with the double-pair event of SPDC, one needs to consider the tradeoff between the detection rate and the multiphoton noise contribution to the data. In our setup, we find that 260-mW pump power results in 2.5%, 0.06%, and 0.002% emission probabilities of a single, double, and triplet pairs, respectively. In case of the states  $|3,0\rangle$  and  $|0,3\rangle$ , on the other hand, the fourfold coincidence probability is half of the state  $\frac{1}{\sqrt{2}}(|3,0\rangle - i|0,3\rangle)$ . Thus, we are able to use twice-high pump power in this case to reduce the measurement time.

Finally, the heralded three-photon state is characterized by performing quantum state tomography using 16 projection measurements set by QWP2, HWP3, and PBS in Fig. 1 and a maximum likelihood estimation [22]. The experimentally obtained density matrices for the representative three-photon states listed in Table I are shown in Fig. 3. Mixed states are obtained by incoherently adding pure states with the proper ratio. The three-photon entangled state  $\frac{1}{\sqrt{2}}(|3,0\rangle - i|0,3\rangle)$  has the lowest fidelity because the triple-pair contribution from pulsed SPDC to the noninterfering background is more noticeable [17,18].

#### IV. ANALYSIS

In this section, we analyze the experimentally generated three-photon polarization states with the central-moment description of quantum polarization up to the third order. (The fourth- and higher-order Stokes moments can be expressed as a function of the lower-order moments.) The central moments, plotted in the corresponding direction on the Poincaré sphere, show quantum polarization features, such as rotation invariants and the polarization uncertainty distribution. For instance, classical unpolarized light is SU(2) rotation invariant, that is,

it is rotationally invariant in all directions on the sphere. If the first  $m$  moments are rotationally invariant, the state is defined to be  $m$ th-order unpolarized [14]. As for the uncertainty relation regarding quantum polarization in Eq. (3b), all three-photon states have a common restriction that the sum of the variances along three orthogonal polarizations on the Poincaré sphere (indicating three complementary polarization bases) is between 6, from  $2\langle\hat{S}_0\rangle$ , and 15, from  $\langle\hat{S}_0\rangle(\langle\hat{S}_0\rangle + 2)$ , because  $\langle\hat{S}_0\rangle = 3$ .

The identity density matrix is invariant of any rotation transformation since  $\hat{\mathbb{I}}/4 = \hat{U}_n^\dagger(\hat{\mathbb{I}}/4)\hat{U}_n$ , where  $\hat{U}_n$  is any SU(2) rotation. So, this state always gives an isotropic expectation value for quantum polarization in any basis. That is, every order of its quantum polarization is rotationally invariant and the state is hence unpolarized to every order. Since the state is first-order unpolarized, the second-order central moment or the variance is given by the mean square of the Stokes operator. As the eigenvalues of  $\hat{S}_3$  for the states  $|3,0\rangle, |2,1\rangle, |1,2\rangle$ , and  $|0,3\rangle$  are 3, 1,  $-1$ , and  $-3$ , respectively, the value  $\langle\hat{\Delta}_3^2\rangle$  for the state  $\hat{\mathbb{I}}/4$  is  $(9 + 1 + 1 + 9)/4 = 5$ . This state has the isotropic variance, so the sum of variance is 15, making it the maximum sum-uncertainty state. As expected, in Fig. 4(a), the experimental result confirms the theoretical results with only small errors. Note that for the odd polarization orders, the illustrated quantity is the absolute value of the moment plotted as a function of the direction  $\mathbf{n}$  on the Poincaré sphere. For odd polarization orders  $m$  it holds that  $\langle\hat{\Delta}_n^m\rangle = -\langle\hat{\Delta}_{-\mathbf{n}}^m\rangle$ .

Any second-order unpolarized three-photon quantum state must be a mixed state, see the proof in [14]. Among the mixed states, the state  $\frac{1}{3}|3,0\rangle\langle 3,0| + \frac{1}{2}|1,2\rangle\langle 1,2| + \frac{1}{6}|0,3\rangle\langle 0,3|$  has the maximum sum-uncertainty. This state is isotropic up to the second order and is polarized in the third order, as shown theoretically and experimentally in Fig. 4(b).

The states  $|3,0\rangle$  and  $|0,3\rangle$  have rotation symmetry about the  $\hat{S}_3$  axis. The symmetry is preserved upon mixing (i.e., incoherent addition of quantum states), and they have vectors in opposite directions from each other on the Poincaré sphere. Therefore, the mixed state  $\frac{1}{2}(|3,0\rangle\langle 3,0| + |0,3\rangle\langle 0,3|)$  has vanishing all odd-order central moments as shown in Fig. 4(c). The second-order central moment is, however, maximized along the  $\hat{S}_3$  axis (with the value of 9) and minimized on the  $\hat{S}_1$ - $\hat{S}_2$  plane (with the value of 3). The state  $\frac{1}{2}(|3,0\rangle\langle 3,0| + |0,3\rangle\langle 0,3|)$  therefore is a three-photon maximum sum-uncertainty state, having the quantum polarization properties of second-order hidden polarization, polarized in the second order, and with no third-order polarization.

Let us now consider the case of the entangled state  $\frac{1}{\sqrt{2}}(|3,0\rangle - i|0,3\rangle)$ . It is clear that some quantum polarization features of the entangled state would be similar to the mixed state  $\frac{1}{2}(|3,0\rangle\langle 3,0| + |0,3\rangle\langle 0,3|)$ , as both contain the same basis states. This is reflected in the first-order and second-order quantum polarization properties. The key difference between the two states is inherent coherence and is reflected on the third-order quantum polarization, producing skewness in three directions as shown in Fig. 4(d). The three-photon NOON state is well known to exhibit  $N$  times phase sensitivity compared to a classical state, and this feature is illustrated in the third-order quantum polarization, showing three oscillations during the  $2\pi$

phase change on the  $\hat{S}_1$ - $\hat{S}_2$  plane. Note that the figure shows the absolute value of central moment. In the experiment, the state is not quite ideal, see the density matrix in Fig. 3(d), so the skewness is somewhat reduced (resulting in a reduced NOON state interference visibility) compared to the theoretical one. Note that the variances  $\langle\hat{\Delta}_1^2\rangle, \langle\hat{\Delta}_2^2\rangle$ , and  $\langle\hat{\Delta}_3^2\rangle$  are calculated to be 3, 3, and 9, respectively. Thus the state is also a maximum sum-uncertainty state. The state has second-order hidden polarization but is polarized to second and third order.

We now consider the state  $\frac{19}{36}|3,0\rangle\langle 3,0| + \frac{15}{36}|1,2\rangle\langle 1,2| + \frac{1}{18}|0,3\rangle\langle 0,3|$ , which is first-order and third-order polarized but with isotropic second-order central moment (see Table I). The theoretical and experimental results shown in Fig. 4(e) illustrate this feature of the state. Note that since the state is a mixture of horizontal and vertical basis eigenstates, it has rotational symmetry about the  $\hat{S}_3$  axis, but it is not a maximal sum-uncertainty state.

Finally, consider the state  $|3,0\rangle$  which is clearly first-order, second-order, and third-order polarized as all three photons are horizontally polarized, and this is shown by the anisotropic features in all orders of central moments in Fig. 4(f). Since the state is an eigenstate of  $\hat{S}_3$ ,  $\langle\hat{\Delta}_3^m\rangle$  vanishes for all  $m$ . Moreover, both  $\langle\hat{\Delta}_1^m\rangle$  and  $\langle\hat{\Delta}_2^m\rangle$  vanish for odd  $m$ . Thus the odd polarization moments all vanish on the  $\hat{S}_1$ - $\hat{S}_2$  plane. Note that the state satisfies (3a) with equality on the  $\hat{S}_1$ - $\hat{S}_2$  plane.

The advantages of using the quantum polarization description of the multiphoton state can be summarized as follows. As evidenced in Fig. 4, the quantum polarization description allows one to visually identify for which applications the quantum state is best suited. For instance, the mixed state  $\frac{1}{3}|3,0\rangle\langle 3,0| + \frac{1}{2}|1,2\rangle\langle 1,2| + \frac{1}{6}|0,3\rangle\langle 0,3|$  shown in Fig. 4(b) can be useful for polarization interferometry involving three-photon correlation measurement. However, the mixed state  $\frac{1}{2}(|3,0\rangle\langle 3,0| + |0,3\rangle\langle 0,3|)$  shown in Fig. 4(c) is better suited for two-photon correlation interferometry due to the anisotropy in the second-order quantum polarization. Also, the NOON state offers the best phase sensitivity to SU(2) rotations, as evidenced in the third-order quantum polarization behavior shown in Fig. 4(d). Note also from Fig. 4(d) that the NOON state offers threefold improvement of phase sensitivity over the classical behavior, as well as the possibility to get unity interference visibility. Such information is not at all evident from the density matrix description of the quantum states shown in Fig. 3, although, for a two-mode state with  $N$  photons, or equivalently, a state of composite system for  $N$  spin-1/2 particles, the two figures contain mathematically equivalent and interconvertible information. Additionally, deviations of the experimental quantum states from their ideal target states are more easily identified in Fig. 4 than in Fig. 3, as it is difficult to deduce such information from a visual inspection of the density matrices in Fig. 3.

## V. CONCLUSION

We have experimentally studied diverse quantum polarization features of different three-photon states, selected to represent the six possible three-photon polarization classes.

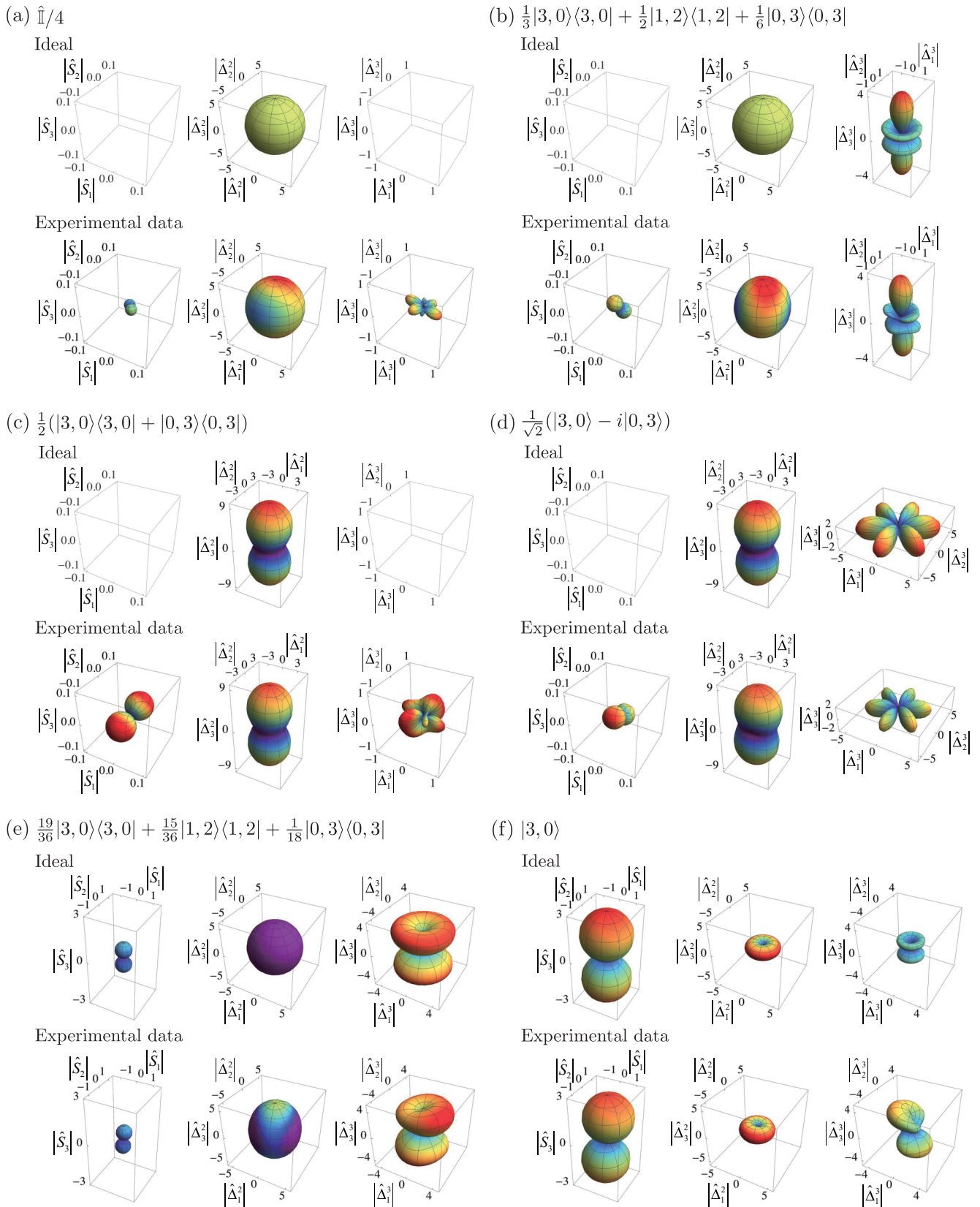


FIG. 4. Central-moment quantum polarization descriptions of assorted three-photon states. The rainbow-colored gradient represents the distance from the origin of the coordinate system. In general, the red color illustrates the farther distance from the origin. Depicted in each panel are, left-to-right, the mean value  $\langle |\hat{S}_n| \rangle$ , the variance  $\langle \hat{\Delta}_n^2 \rangle$ , and the absolute value of the skewness  $\langle |\hat{\Delta}_n^3| \rangle$ . Note that for odd polarization orders  $m$ ,  $\langle \hat{\Delta}_n^m \rangle = -\langle \hat{\Delta}_{-n}^m \rangle$  and thus the illustrated quantity is the absolute value of the moment plotted as a function of the direction  $\mathbf{n}$  on the Poincaré sphere.

The states have interesting characteristics such as perfect polarization, absence of polarization, hidden polarization, and maximum sum-uncertainty. Our classification and experimental results for three-photon states can be applied as well to describe the spin features of composite systems consisting of three spin-1/2 particles with the bosonic characteristic. In addition, we have shown that subtle quantum polarization features are more sensitive to state imperfections than those of state density matrices. Our results hint that the central-moment description can be used to describe the quality of a multiphoton polarization state with better sensitivity, particularly in cases where higher-order polarization features are important.

### ACKNOWLEDGMENTS

This work was supported by the National Research Foundation of Korea (Grants No. 2016R1A2A1A05005202, No. 2016R1A4A1008978, and No. NRF-2012K1A2B4A01033433). Y.K. acknowledges support from the Global Ph.D. Fellowship by the National Research Foundation of Korea (Grant No. 2015H1A2A1033028). G.B. acknowledges financial support by the Swedish Foundation for International Cooperation in Research and Higher Education (STINT) Contract No. 2012-2066, the Swedish Research Council (VR), through its Linnaeus Center of Excellence ADOPT Contract No. 621-2014-5410.

- 
- [1] P. G. Kwiat, K. Mattle, H. Weinfurter, A. Zeilinger, A. V. Sergienko, and Y. Shih, *Phys. Rev. Lett.* **75**, 4337 (1995).
- [2] M. Ringbauer, B. Duffus, C. Branciard, E. G. Cavalcanti, A. G. White, and A. Fedrizzi, *Nat. Phys.* **11**, 249 (2015).
- [3] T. Schmitt-Manderbach, H. Weier, M. Fürst, R. Ursin, F. Tiefenbacher, T. Scheidl, J. Perdigues, Z. Sodnik, C. Kurtsiefer, J. G. Rarity, A. Zeilinger, and H. Weinfurter, *Phys. Rev. Lett.* **98**, 010504 (2007).
- [4] K. Mattle, H. Weinfurter, P. G. Kwiat, and A. Zeilinger, *Phys. Rev. Lett.* **76**, 4656 (1996).
- [5] Y.-H. Kim, S. P. Kulik, and Y. Shih, *Phys. Rev. Lett.* **86**, 1370 (2001).
- [6] E. Martín-López, A. Laing, T. Lawson, R. Alvarez, X.-Q. Zhou, and J. L. O'Brien, *Nat. Photonics* **6**, 773 (2012).
- [7] G. G. Stokes, *Trans. Cambridge Philos. Soc.* **9**, 399 (1852).
- [8] P. Usachev, J. Söderholm, G. Björk, and A. Trifonov, *Opt. Commun.* **193**, 161 (2001).
- [9] L. K. Shalm, R. B. A. Adamson, and A. M. Steinberg, *Nature (London)* **457**, 67 (2009).
- [10] A. B. Klimov, G. Björk, J. Söderholm, L. S. Madsen, M. Lassen, U. L. Andersen, J. Heersink, R. Dong, Ch. Marquardt, G. Leuchs, and L. L. Sánchez-Soto, *Phys. Rev. Lett.* **105**, 153602 (2010).
- [11] G. Jaeger, M. Teodorescu-Frumosu, A. Sergienko, B. E. A. Saleh, and M. C. Teich, *Phys. Rev. A* **67**, 032307 (2003).
- [12] U. Schilling, J. von Zanthier, and G. S. Agarwal, *Phys. Rev. A* **81**, 013826 (2010).
- [13] J. Söderholm, G. Björk, A. B. Klimov, L. L. Sánchez-Soto, and G. Leuchs, *New J. Phys.* **14**, 115014 (2012).
- [14] G. Björk, J. Söderholm, Y.-S. Kim, Y.-S. Ra, H.-T. Lim, C. Kothe, Y.-H. Kim, L. L. Sánchez-Soto, and A. B. Klimov, *Phys. Rev. A* **85**, 053835 (2012).
- [15] Ö. Bayraktar, M. Swillo, C. Canalias, and G. Björk, *Phys. Rev. A* **94**, 020105(R) (2016).
- [16] P. Kok, H. Lee, and J. P. Dowling, *Phys. Rev. A* **65**, 052104 (2002).
- [17] H. Kim, H. S. Park, and S.-K. Choi, *Opt. Express* **17**, 19720 (2009).
- [18] Y.-S. Kim, O. Kwon, S. M. Lee, J.-C. Lee, H. Kim, S.-K. Choi, H. S. Park, and Y.-H. Kim, *Opt. Express* **19**, 24957 (2011).
- [19] W. P. Grice, A. B. U'Ren, and I. A. Walmsley, *Phys. Rev. A* **64**, 063815 (2001).
- [20] C. O. Alley and Y. H. Shih, in *Proceedings of the Second International Symposium on Foundations of Quantum Mechanics in the Light of New Technology* (Physical Society of Japan, Tokyo, 1986), pp. 47–52; Y. H. Shih and C. O. Alley, *Phys. Rev. Lett.* **61**, 2921 (1988).
- [21] C. K. Hong, Z. Y. Ou, and L. Mandel, *Phys. Rev. Lett.* **59**, 2044 (1987).
- [22] Y. Israel, I. Afek, S. Rosen, O. Ambar, and Y. Silberberg, *Phys. Rev. A* **85**, 022115 (2012).